Rev. Adv. Mater. Sci. 47 (2016) 95-104

THERMAL EVOLUTION OF THE MICROSTRUCTURE OF CALCIA STABILIZED ZIRCONIA PRECURSORS MANUFACTURED BY CRYOCHEMICAL TECHNIQUE

O.Yu. Kurapova[1,2], D.V. Nechaeva[1], A.V. Ivanov[1], S.N. Golubev[2], V.M. Ushakov[2] and V.G. Konakov[1,2]

[1]St. Petersburg State University, St. Petersburg, 199034, Russia
[2]Glass and Ceramics Ltd., St. Petersburg, 199004, Russia

Received: November 06, 2016

Abstract. The work reports the evolution of nanosized *x*CaO-(100-*x*)ZrO_2 precursors, where *x* = 9-15 mol.% manufactured by the original cryochemical technique including co-precipitation and freeze-drying or gels freezing in liquid nitrogen. Basing on the results of SEM, BET, and PSD analysis, it was shown that the way of dehydration and the amount of CaO affect the pore size and precursor morphology. The systematic investigation performed by BET, TG, and XRD allowed to reveal the features of microstructural evolution of the precursors up on their annealing in the temperature range 400-1300 °C and to indentify the processes governing the transformation of amorphous sponge-type structure to globular crystalline one. It was found that specific surface area of the precursors after freeze-drying and freezing in the liquid nitrogen is ~1.5 times lower than in the case of the conventional evaporation techniques.

1. INTRODUCTION

Due to their high ionic conductivity and transfer numbers close to 1 at 800-1100 °C, cubic zirconia solid solutions found their wide application in various electrochemical devices, and, in particular, as solid electrolytes (SE) used as membranes for oxygen sensors manufacturing [1-4]. Yttria based zirconia ceramics ($8Y_2O_3$-$92ZrO_2$, known as YSZ) is usually utilized as a membrane material. The efficiency of in situ oxygen monitoring in different medias depends both on physical, chemical, and transport properties of the membrane and working temperature of the sensor [5-7]. The life cycle of these sensors in a corrosive atmosphere at high temperatures is rather small due to slow degradation of the ceramic membrane. That is why novel materials are actively researched as an alternative to YSZ ceramics. As it was shown in [8], the use of nanosized zirconia based precursors for solid electrolytes fabrication allows the improvement of the ceramic membrane properties. However, the applicability of these precursors is limited by a number of requirements: the necessity of cubic zirconia solid solution stabilization, high powders dispersity, powders, low powders agglomeration degree, etc. An important aspect defining the possibility of vacuum dense ceramics fabrication for electrochemical devices is the low specific surface area and low open porosity of agglomerates in powders. The combination of sol-gel reversed co-precipitation technique and unidirectional freezing such as freeze drying and liquid nitrogen treatment is an effective way to manufacture dense precursors with required physical and chemical properties. In general, gels obtained by various sol-gel techniques can be subjected to freeze drying; the choice of the freeze drying regimes provides the production of micro- and nanoparticles

Corresponding author: O.Yu. Kurapova, e-mail: olga.yu.kurapova@gmail.com

with different porosity, morphology, the size and the shape of pores in agglomerates. Recent reviews describing cryochemical dehydration, freeze-drying, and freeze-casting are mainly addressed to potentialities and challenges of highly porous ceramic materials manufacturing that have irregular i.e. cellular, lamellar, or of even more complex dendritic morphologies or regular i.e. aligned pore structure. Inorganic precursors are usually produced by freeze-drying of freshly precipitated aqueous gels, sols, and even suspensions obtained by mixing of commercial powders and water. Large surface area of such ceramics provides a large number of reaction sites which allows using it as catalyst support [9,10]. Non-aqueous media (alcohols, tetrahydrofuran, campene, etc.) are actively implicated for the manufacturing of porous hydrophobic biodegradable materials suitable as scaffolds for tissue engineering or for materials for targeted drug delivery [9-12]. In addition, freeze-drying is actively used for the dehydration of slurries based on various solvents during molding of the ceramic pieces and green bodies of complicated geometry. Some authors point out the bright possibility of freeze-drying and related cryochemical dehydration techniques for nanosized zirconia powders fabrication [13-15]. However, the systematic study of the effect of cryochemical dehydration on the microstructure dispersity of zirconia powders for further SE manufacturing was not still performed. As it was mentioned in [11], the versatility of the process allows considering a wide range of technical ceramics and composites with the typical dimensions being suitable for applications in solid oxide fuel cells (SOFC) in sensors and actuators. Thus, the goal of the present work is the characterization of the nanosized zirconia precursors obtained by reverse co-precipitation and further unidirectional freezing; microstructure evolution, specific surface area, crystallite size, and phase formation of these precursors were studied in the temperature range 400-1300 °C.

2. EXPERIMENTAL

2.1. Synthesis

Nanosized calcia stabilized zirconia powders were obtained by reverse co-precipitation from diluted aqueous salt solutions. The compositions with CaO content 9, 12, and 15 mol.% (compositions I, II and III, respectively) were chosen accounting for CaO-ZrO_2 phase diagram [16]. In order to prepare 0.1M aqueous solution, commercially available hydrates $ZrO(NO_3)_2{\cdot}2H_2O$ and $Ca(NO_3)_2{\cdot}2H_2O$ were used. 1M ammonium aqueous solution was used as a precipitant. Mixed salt solution was added to NH_4OH by drops with a rate of ~ 2 ml/min. The precipitation has been performed at ~1-2 °C in an ice bath at stirring; pH of the solution was kept at ~9-10 during the synthesis by ammonium solution addition. To remove reaction byproducts, the obtained gels were filtered and rinsed until the neutral pH was reached. The obtained gels underwent different unidirectional freezing via freeze-drying and freezing in liquid nitrogen (treatment 1 and 2, respectively).

Freeze-drying (1). The freeze-drying conditions for nanosized precursors fabrication were optimized in [17] by use of simultaneous thermal analysis (STA) and particle size distribution analysis (PSD-analysis). Thin layer of gels I, II, and III were deposited to Petri dish surface and then rapidly frozen at -50 °C, the cooling rate here was ~1-2 °C/min. The frozen gels were then freeze-dried in Labconco 1l chamber at 0.018 Torr and 20 °C for 24 hours.

Freezing in liquid nitrogen (2). To perform freezing in liquid nitrogen, freshly precipitated gel, was placed by small portions into a Dewar flask with liquid nitrogen under mechanical stirring. The stirring is necessary to reach homogeneous gel freezing since the layer of solidified gel is formed on the surface of the liquid nitrogen that blocks the contact of liquid N_2 and next portions of the gel. After the liquid nitrogen evaporation, the frozen granules were left at the ambient conditions in order to evaporate water and obtain powder.

At the final step of sample manufacturing, all precursors obtained were annealed at 400, 600, 800, 1000, and 1300 °C during 3 hours.

2.2. Analysis

Microstructure of samples surface was investigated by scanning electron microscopy (SEM, Hitachi S-3400N). Thermal gravimetric (TG) analysis was performed using STA 449 F1 Jupiter Netzsch in nitrogen ambience, the heating rate here was 10 °C/min. Phase composition of the precursors after synthesis and annealing was identified using X-ray diffraction analysis (Cu-Kα radiation, λ = 1.54 Å, room temperature). The data on precursors specific surface area was obtained using BET technique (Brunauer-Emmet-Teller, ASAP 2020MP Micromeritics). The mean size of crystallites was estimated via Scherrer's equation using the profile of the peak at 2θ = 29.5° and using BET data according to Eq. (1):

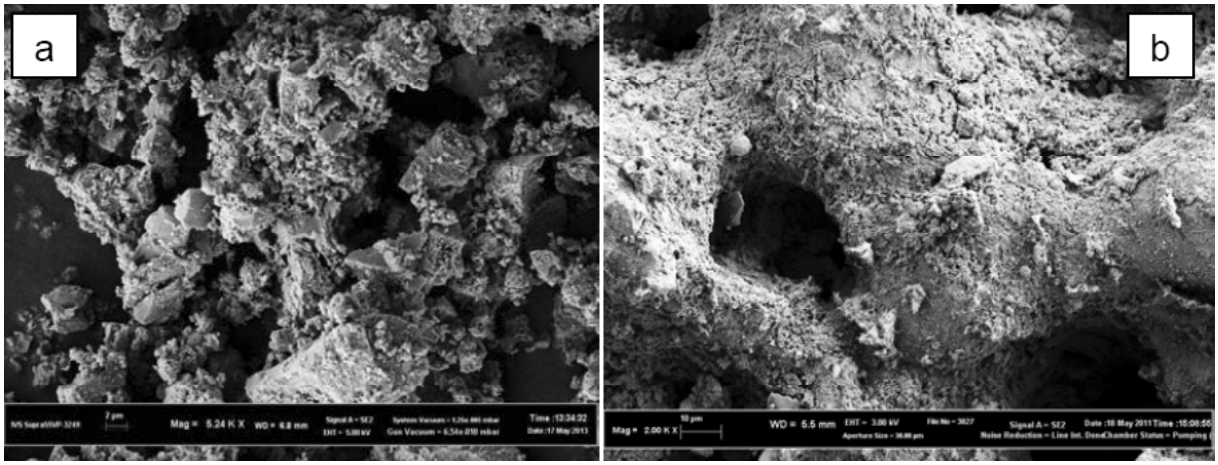

Fig. 1. SEM data for precursor I obtained by a) freezing of gel in the liquid nitrogen (2) and b) freeze-drying of gel (1)**.**

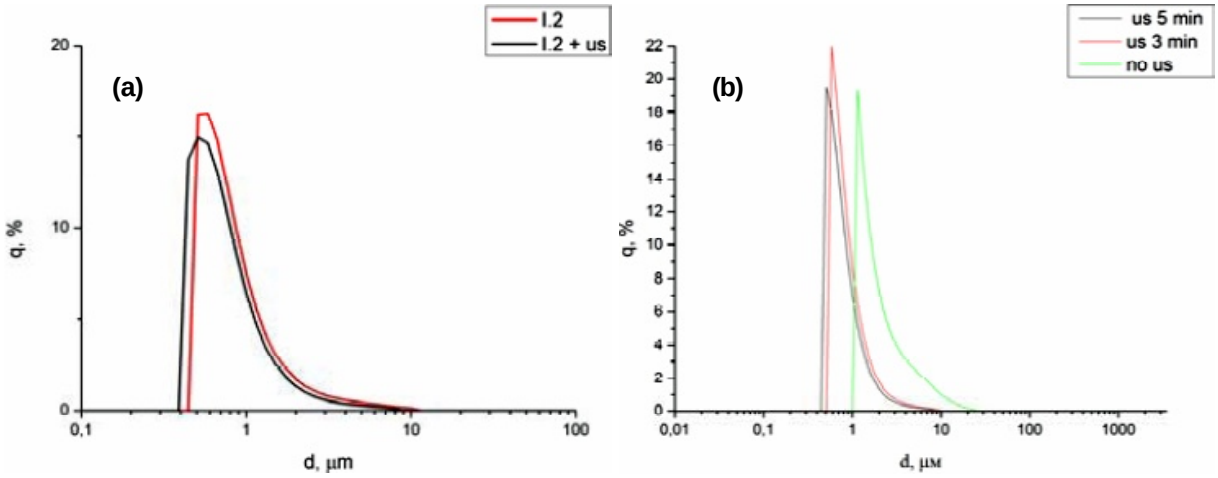

Fig. 2. Particle size distribution of agglomerates “by size” in precursor I a) freezing of gel in the liquid nitrogen (2) and b) freeze-drying of gel (1) with the use of ultrasound and without**.**

$$d_{BET} = \frac{6 \cdot 10^{-3}}{\rho S_{BET}}, \qquad (1)$$

where d_{BET} is a diameter of spherical crystallite (nm), ρ is the theoretical density of the phase (the of cubic zirconia phase density of 5.269 g/cm^3 was used in the current work), S_{BET} is the surface area calculated according to BET theory, m^2/g. Mesopores size distribution as well as the data on pore volume were calculated using BJH (Barrett-Joyner-Halenda) theory, corresponding data for micropores were calculated by (Horvath-Kawazoe) HK theory.

3. RESULTS AND DISCUSSION

Typical microstructure of precursors after unidirectional freezing is presented in Fig. 1. As seen from the figure, dehydration by both freeze-drying and freezing in liquid nitrogen results in rather dense sponge type structure formation, which is generally typical for all zirconia based precursors obtained by sol-gel techniques [18]. However, the dehydration technique affects the precursor morphology and particle agglomeration degree of the dispersed phase. Precursor I.2, obtained by the freezing of gel in the liquid nitrogen (see Fig. 1a) is composed of dendritic agglomerates with a random size. Indeed, agglomerate size in this powder according to PSD analysis (see Fig. 2a) varies in the range from 0.45 to 10 μm, the mean agglomerate size is ~0.65 μm. In contrast, precursor I.1 after freeze-drying is a three-dimensional (3D) macroporous network composed of agglomerates with a mean size ~0.96 μm (see Figs. 1b and 2b). Macropores are the replica of large hexagonal ice crystals of dispersed medium removed by sublimation during freeze drying. Due to the fact that dehydration process takes place directly from solid to gas, a number of contacts between the particles of the

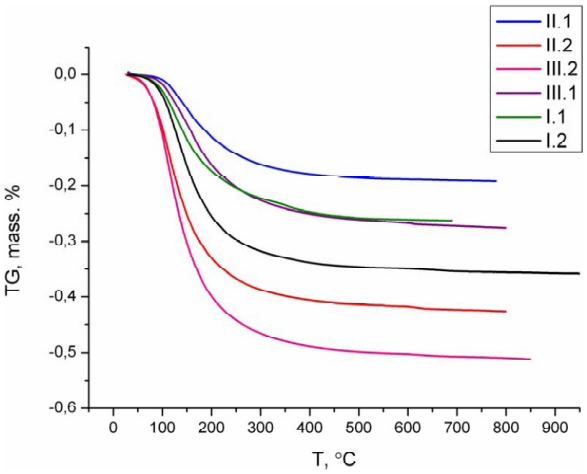

Fig. 3. TG data obtained for precursors I, II, and III, where 1 is referred to freeze-drying and 2 – to freezing in liquid nitrogen.

dispersed phase significantly decrease and the agglomeration becomes eliminated.

Similarly to precursor I.2, precursor I.1 consists of fine agglomerates. However, the number of agglomerates with the size less than 1 μm in case of freeze-dried precursors is higher than that in case of drying in the liquid nitrogen. In general, the agglomerates formed in both dehydration techniques are not stable and can be easily broken by mechanical impact, for example, by ultrasound. Mean agglomerate size in the freeze-dried precursor decreases in ~1.5 times reaching 630 nm. Similar results were obtained for compositions II and III.

Fig. 3 illustrates TG data obtained for precursors I, II, and III after freeze-drying and treatment in liquid nitrogen. One can see that the heating of the precursors up to 900 °C, regardless to their composition, is accompanied by significant mass losses. Since ~90% of mass loss takes place at temperatures below 400 °C, the process can be referred as simultaneous water losses of dispersed and structural water according to schematic sequence of reactions:

$$x\,Ca(OH)_2 \cdot (100-x)\,Zr(OH)_4 \cdot n\,H_2O \rightarrow x\,Ca(OH)_2 \cdot (100-x)\,Zr(OH)_4 + n\,H_2O, \quad (2)$$

$$Zr(OH)_4 \rightarrow ZrO(OH)_2 + H_2O\ (\sim 140\ ^\circ C), \quad (3)$$

$$ZrO(OH)_2 \rightarrow ZrO_2 + H_2O, \quad (4)$$

$$Ca(OH)_2 \rightarrow CaO + H_2O\ (\sim 550\ ^\circ C). \quad (5)$$

Since the removal of structural water from $Zr(OH)_4$ due to gel to sol transition begins already at ~140 C and the formation of CaO from $Ca(OH)_2$ takes place just at ~550 °C [19], it is reasonable to assume that total mass losses at temperatures ≤400 °C are mainly due to $Zr(OH)_4$ dehydtation. That conclusion is in accordance with literature data on ziconia precursors dehydration [21]. The additional step on TG curves is observed at ~530-580 °C for some precursors. That small mass loss can be attributed to powder density increase upon the crystallization of the amorphous precursors resulting in cubic zirconia solid solution formation.

Total mass losses (calculated per one mole) for all the samples at temperatures below 400 °C are summarized in Table 1 and compared with the theoretical water losses by xCa(OH)$_2$·(100-x)Zr(OH)$_4$ hydroxides, x = 0.09, 0.12, 0.15. As follows from the table, the experimental mass losses for all the compositions exceed theoretical. In particular, the total mass losses for all freeze-dried precursors are less than ~30 g/mol, whereas that value after freezing in liquid nitrogen lies in the range ~40-56 g/mol. Note that the use of freeze-drying and freezing in liquid nitrogen can be considered as a nondestructive way of dehydration. Indeed, the use of these techniques allows retaining the structural water in hydroxides, i.e. the initial structure and dispersity

Table 1. Mass loss by calcia stabilized zirconia precursors calculated from TG data at temperatures ≤400 °C, g/mol.

Sample number	Experimental data	Theoretical estimates for xCa(OH)$_2$(100-x)-Zr(OH)$_4$ hydroxides
I.1	29.86	26.82
I.2	40.35	
II.1	26.54	26.49
II.2	48.17	
III.1	28.80	26.09
III.2	55.62	

of gels obtained by reversed co-precipitation is preserved.

The analysis of XRD results indicated that all the precursors after synthesis and dewatering are X-ray amorphous. The further annealing of the precursors at 400-1300 °C allows establishing the effect of annealing temperature and precursor composition on phase formation.

Dehydration technique significantly affects on the phase formation in the precursors. In case of freeze-dried precursors I-III, the crystallization onset takes place already at 400 °C, whereas samples obtained by gel freezing in liquid nitrogen and drying at room temperature are still X-ray amorphous at this temperature. In general, phase evolution follows empiric Ostwald step rule: metastable phase (or a series of metastable phases) comes prior the thermodynamically stable phase. In case of zirconia precursors, the most symmetric cubic zirconia solid solution appears to be a direct result of amorphos precursors crystallization. As the crystallinity value after annealing at 600 °C is 50-58%, solid solution formed could be considered as low-crystalline. Temperature and concentration range of cubic solid solution phase stabilization determined for the synthesized samples significantly differ from CaO-ZrO_2 phase diagram data for microsized particles [16], but rather are quite similar to the reference data for zirconia precursors obtained by sol-gel techniques [1,2]. According to [16], the lowest CaO content required for cubic solid solution stabilization is 12 mol.%. In the present work, the cubic solid solution without the admixture of low symmetric phases (monoclinic or tetragonal zirconia) is observed already for compostion I with 9 mol.% content of CaO. On the contrary, the formation of cubic solid solution in case of composition III (15 mol.% CaO) is accompanied by traces of monoclinic phase, its content can be estimated as 3-6 %. The increase in annealing temperature favors slow crystallinity increase, however, the crystallinity after the annealing at 1000 °C does not exceed 77%. That allows stating the phase stabilization of solid solution formed. Phase stabilization of cubic zirconia solid solution without any admixtures is observed at annealing temperatures up to 1000 °C for precursor II.2 after freezing in liquid nitrogen.

The observed phase evolution behavior can be explained from the point of view of residual OH-groups presence in the structure up to high temperatures [16]. Further temperture increase results in the transformation of cubic solid solution into monoclinic phase or a mixture of monoclinic and tetragonal phases. The precursors composition at 1000 °C tends to thermodynamically stable.

Let us consider the microstructure of powders in more detail. Adsorption-desorption curves obtained for freeze-dried precursors I and II with 12 and 15 mol.% CaO content are referred to V-type of adsorption isotherms (see Fig. 3a) [18]. The form of the isotherms gives the evidence to the weak adsorbent-adsorbate interaction, it is typical for amorphous transient hydroxides with cylindrical pores having sponge-like structure. This conclusion agrees with SEM observations (see Fig. 1). As it is seen from Fig. 4a, the hysteresis loop observed for freeze-dried precursors is rather small indicating the almost full absence of mesopores in a sample structure. The adsorption is mainly due to the fact that adsorbate fills free space between the particles of the dispersed phase because of their loose packing. That assumption can be confirmed by the PSD data consideration obtained for freeze-dried powder II.1. Indeed, as it is seen from pore distribution on their volume (see Fig. 5a), the pore volume in freeze-dried powder before annealing does not exceed 0.003 cm^3/g and the linear size lies in the range 2-5 nm, most pores are characterized by linear size of 2-3 nm.

It is intersting to note that BET isotherms were not obtained in case of precursor with 15 mol.% CaO content and precursors after freezing in the liquid nitrogen. Latter is likely due to powders microporosity. In order to confirm that assumption made for precursors I.2, II.2, III.1, and III.2, the adsorption-desorption curves were obtained using Krypton as an adsorbate gas. Further modeling according to the density functional theory (DFT) using the approach described in [22] allowed to show that the samples are microporous and their specific surface area lies in range 170-180 g/cm^2.

In general, similar adsorption-desorption curves were obtained for all precursors after different cryochemical dehydration and annealing at 400-800 °C (see Figs. 4b-4d and 6). The annealing at 400 °C results in the increase in the hysteresis loop area which is related to slow dehydration process in the precursors confirmed by TG data (see Fig. 3 and Table 1). Since the crystallization processes in the powders take place at 400-600 °C (see Table 2) and the main mass losses due to dehydration are in the temperature region ≤400 °C, it is reasonable to assume that the further increase in hysteresis loop area after 600 °C is caused by crystallization of cubic solid solution and crystallinity increase (see Table 2). Upon the increase of the annealing temperature

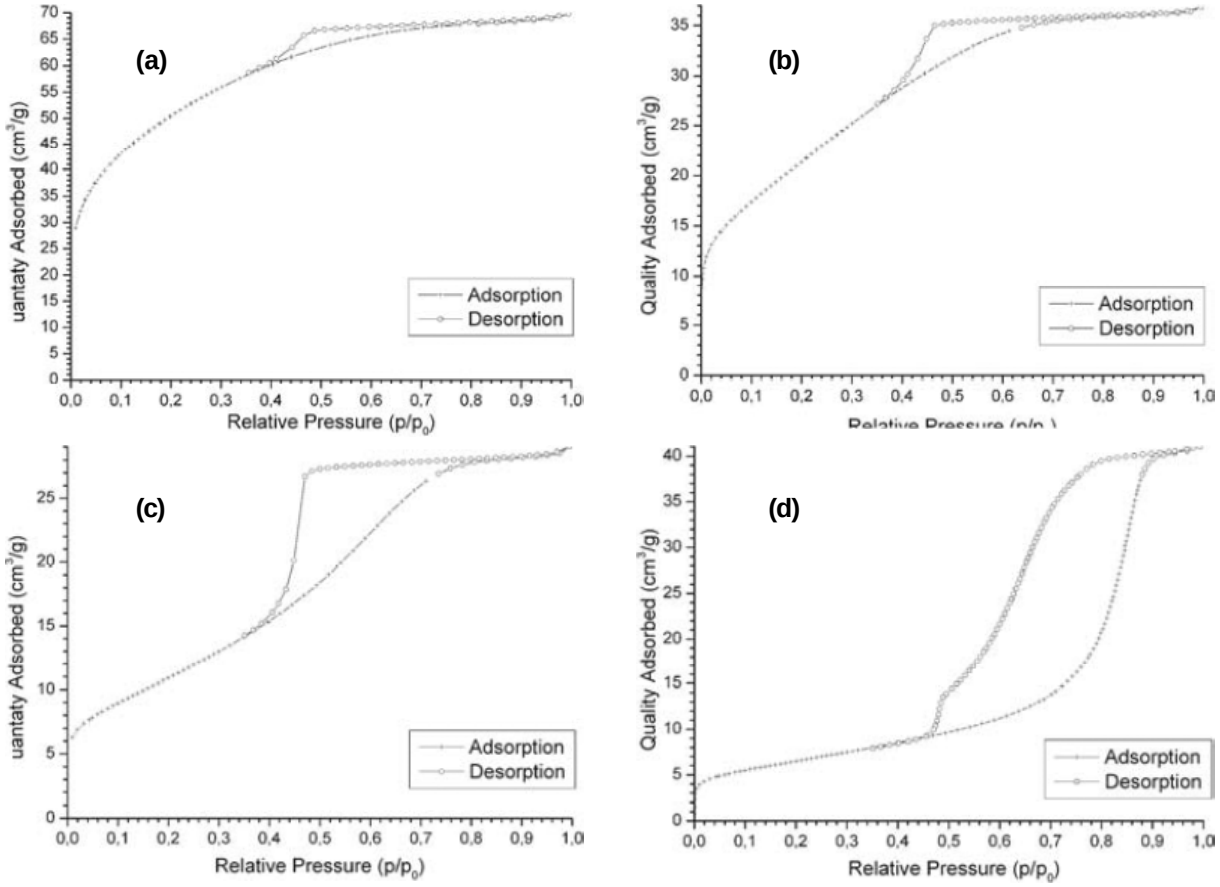

Fig. 4. Adsorption-desorption curves of precursors I and II after freeze drying: a) with no annealing and after the annealing at b) 400, c) 600, and d) 800 °C.

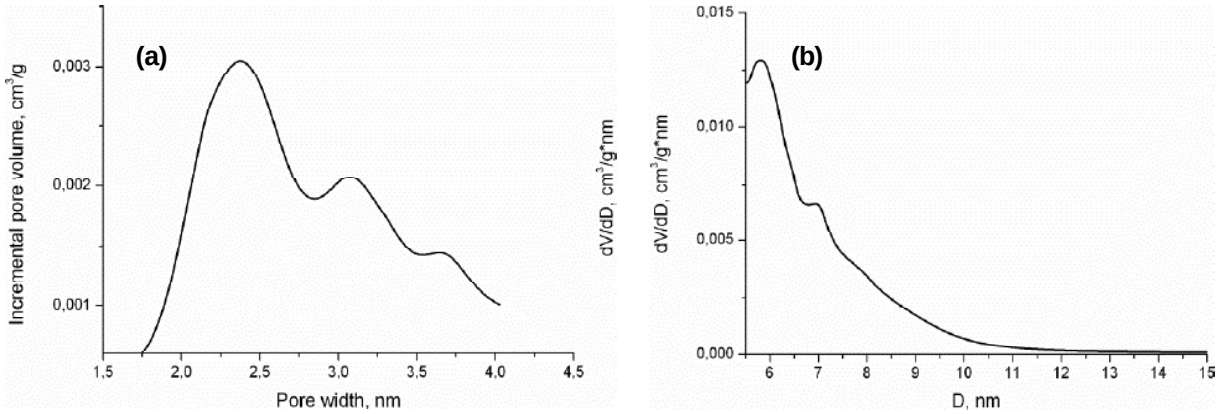

Fig. 5. Pore volume distributions calculated according to BJH theory in precursor II.1 after a) synthesis and b) annealing at 800 °C.

up to 800 and 1000°C (see Figs. 4d, 6b, and 7), the form of adsorption-desorption curves is changed to IV-type. That type of isotherms indicates the globular mesoporous structure formation. From the differential volume pore distribution for freeze dried precursor II.1 (see Fig. 5b), one can see that the annealing results in more ordered structure formation with the pores of 5 and 7 nm. It should be noted that the equilibrium has not been reached in case of all precursors after freezing in liquid nitrogen and freeze-dried precursor III.1 annealed at 1000 °C. That indicates negligibly low values of specific surface area in these precursors and crystallization processes completion, this fact is in accordance with data reported in [8]. The evolution of the specific surface area (*S*) of the precursors with the annealing temperature is shown in Fig. 8.

The specific surface area of freeze-dried and frozen in the liquid nitrogen precursors is 180-200 m^2/g. The obtained value is significantly lower than

Table 2. Phase composition and crystallinity (indicated in brackets) of precursors I-III after annealing at 400-1300 °C, where a – amorphos phase, beg. of cryst. – the beginning of crystallization, c – cubic zirconia solid solution, t – tetragonal zirconia, m – monoclinic zirconia (baddeleite).

T, °C composition	400	600	800	1000	1300
I.1	c (49)	c (55)	c (61)	c+t traces (72)	c:m=70:30 (63)
I.2	beg. of cryst.	c (54)	c (62)	c+t traces (72)	c:m:t=80:10:10 (75)
II.1	beg. of cryst.	c+m traces (58)	c+m traces (67)	c+m traces (76)	c:m=70:30 (69)
II.2	a	c (55)	c (56)	c+m traces (77)	c:m=75:25 (76)
III.1	beg. of cryst.	c+m (50)	c+m (60)	c+m (71)	c:m=70:30 (76)
III.2	a	c+m traces (58)	c+m traces (64)	c+m (74)	c+m =85:15 (83)

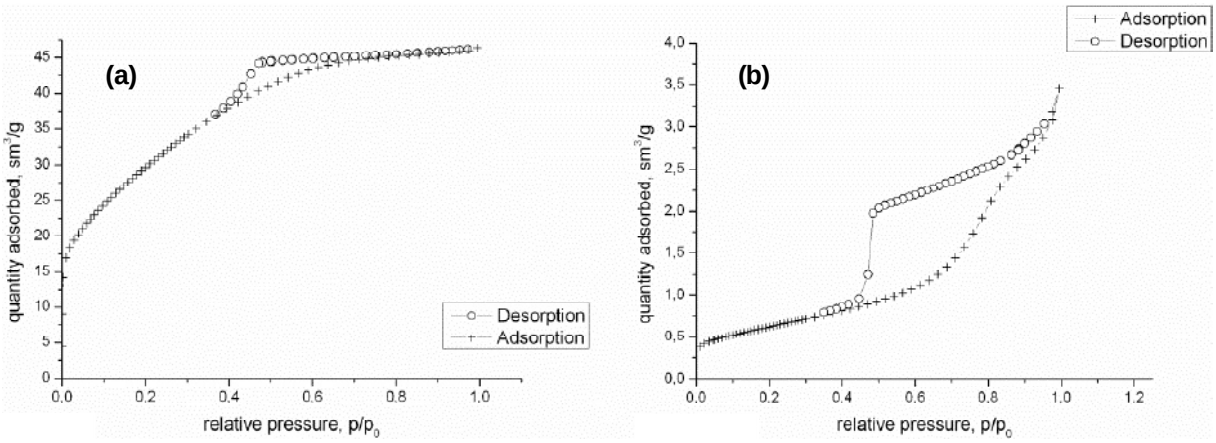

Fig. 6. Adsorption-desorption curves typical for precursors after liquid nitrogen treatment and freeze dried precursors of composition III after freeze-drying and annealing at (a) 400 and (b) 800 °C.

the literature data [23,24] for stabilized zirconia powders obtained by evaporative drying (260-300 m^2/g). According to [18], the observed difference is due to residual water left in freeze-dried powders and precursors after freezing in the liquid nitrogen which is confirmed by TG data. On the other hand, adsorbate, i.e. nitrogen molecules, is adsorbed not only in the mesopores, but also penetrates into the free space between the particles. The lower powder dispersity (i.e. the wider particle size distributions) here results in the higher free volume between the particles. Indeed, freeze-dried precursors according to PSD data are characterized by rather narrow particle size distributions (see Fig. 2). The dense packing due to similar agglomerate size in nanosized powders and the negligible amount of mesopores also contribute into the specific surface area decreas.

The type of S_{BET} temperature dependences is a function of composition and dehydration method. Only two values of specific surface area were obtained (after annealing at 400 and 600 °C) in case of precursors frozen in the liquid nitrogen. That is, most likely, due to discussed microporosity of the agglomerates in precursors and rather sharp decrease of S_{BET} with annealing temperature. The comparison of S_{BET}, TG, and XRD data allows concluding that thermal treatment of powders obtained by cryochemical methods is accompanied by dehydration and initial 3-dimentional porous network of amorphous hydroxides restructuring towards more ordered powder characterized by

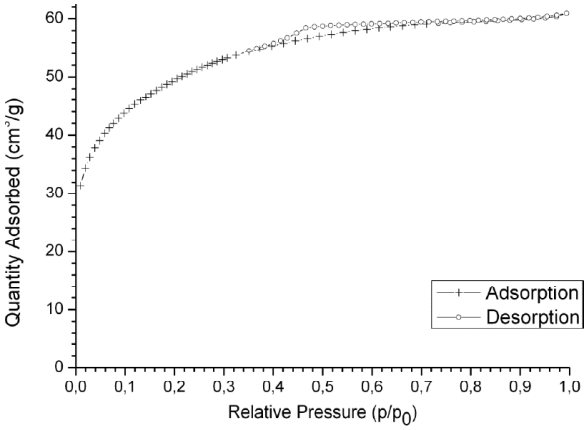

Fig. 7. Adsorption-desorption curves of precursor II.2 annealed at 1000 °C.

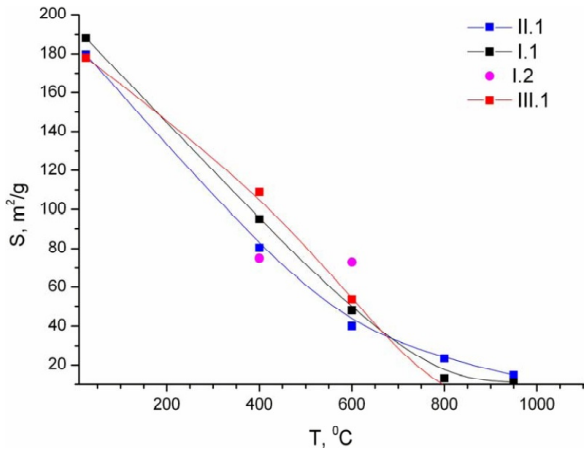

Fig. 8. The dependence of specific surface area of precursors I, II, and III after cryochemical dehydration on the annealing temperature.

lower agglomeration. Two sections that differ by their slope to the horizontal axis are observed in curves III.1 and III.2. The fact that about 90% of the specific area decrease is observed at annealing temperatures d”800 °C allows dehydration, crystallization, and de-agglomeration being simultaneous. The S_{BET} decrease to zero already at 800 °C (see curve III.1 in Fig. 8) indicates that these processes are accompanied by dense crystalline particles formation possessing low open porosity and close packing. Indeed, the fast freezing taking place at both the liquid nitrogen temperature and freezing prior freeze-drying (characterized by the cooling rate > 10 °C/min), the freezing rate overcomes the diffusion rate of particles in gel under its freezing. At these freezing conditions, the particles of the dispersed medium can not redistribute in the gel and push out the crystals of pure disperse medium (water). Further dehydration results in soft agglomerates formation having loose structure which is similar to the initial gel structure observed by SEM. The increase in the annealing temperature leads to the dehydration first on the agglomerate surface and then in the bulk. The process is accompanied by quasi-linear agglomerates growth. The residual specific area falling is evidently related to the residual hydroxyl groups removal from the bulk of the particles and does not provide the reliable information on precursor structure. The conclusion is in accordance with data of [15] reporting that the dehydration in zirconia precursor ends just at 1100 °C.

The dependences of mean crystallite size estimated via Scherrer's equation on the annealing temperature are demonstrated in Fig. 9. Mean crystalline size was also estimated using S_{BET} data, the obtained results (d_{XRD} and d_{BET}, respectively) for precursors III.1 and III.2 are shown in Table 3. As seen from Table 3 and Fig. 9, the precursors are nanocrystalline. The tendency to quasi-linear crystalline growth in the powders after different cryochemical treatment is similar for both estimations. Analyzing the data obtained, one can see that the use of freeze-drying and freezing in the liquid nitrogen allows to minimize the effect of powders composition on the final physical and chemical properties of powders. Both of these techniques based on the phase transition from solid to gas and neither involves any chemical reaction nor brings any impurities into the sample. As a result, the powders of different compositions possess the same structure and agglomerate size. The initial structural similarity obtained, i.e. similar mean agglomerate size and specific surface area values, governs similar precursor evolution processes, i.e. close temperature of crystallization, specific area, and crystallite size growth.

As it is seen from Fig. 9, crystallization processes proceeds slowly resulting in the estimated crystallite size lower than 30 nm for the

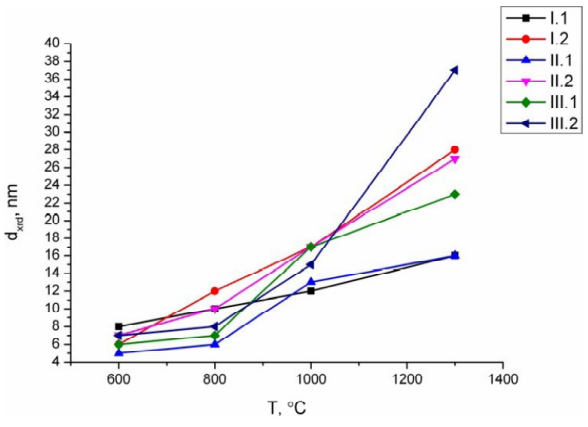

Fig. 9. Crystallite size evolution in precursors with the annealing temperature.

Table 3. Crystallite size (nm), estimated by Scherrer's equation and BET theory for precursors III.1 and III.2.

		400 °C	600 °C	800 °C
III.1 Freeze-dried	d_{BET}	15	15	18
powder	d_{xrd}	5	10	10
III.2 Powder after	d_{BET}	11	22	-
freezing in liquid nitrogen	d_{xrd}	<5	8	9

whole annealing temperature range from 400 to 1300 °C. Similar dependencies, characterized by quasi-linear crystallites growth with temperature were obtained In all cases. However, the plateau at 600-800 °C is observed for freeze-dried powders. Freeze-drying causes prolonged crystallization which is also confirmed by low crystallinity increase with the annealing temperature (see Table 2). Visible increase in crystalline growth rate is observed for precursor III.2 only up on the temperature increase from 1000 to 1300 °C. According to XRD data, the observed difference is likely due to phase composition difference appearing at elevated annealing temperatures.

Summarizing the above STA, XRD, BET, and PSD-analysis data, a number of conclusions on microstructral evolution of the precursors obtained by freeze-drying and freezing in the liquid nitrogen can be stated with regard to further annealing regimes: the evolution of sponge-type 3D porous structure to the globular comprised of small crystallites (~20 nm) at the annealing temperatures ≤800 °C is due to the prolonged dehydration and crystallization that take place simultaneously. Crystallization of the amorphous precursor for all investigated compositions and dehydration techniques is accompanied by cubic zirconia based solid solution formation. Surface area decrease at annealing temperatures from 800 to 1000 °C is due to the residual water losses resulting in the close packing of crystalline particles having low open porosity. The traces of monoclinic and tetragonal zirconia phases are observed for precursors II.1 and III.2. Phase composition at 1000-1300 °C tends to equilibrium [16] which is accompanied by crystallite growth up to 30 nm.

4. CONCLUSIONS

The use of freeze-drying for gels dehydration results in continuous 3D sponge-type mesoporous structure comprised of closely packed agglomerates with the typical linear dimensions of 600-650 nm with mean pore size of 2-3 nm. The increase of CaO amount up to 15 mol.% leads to mesoporous structure transformation to microporous. Freezing in the liquid nitrogen for all the compositions results in sponge-type microporous dendric agglomerates. The increase in the annealing temperature from 400 to 1300 °C fives rise to the evolution of sponge-type structure to the globular comprised of small crystallites (~20 nm) due to simultaneous dehydration, crystallization, and slow crystallites growth. The initial structural similarity of the precursors obtained by cryochemical dehydration (sponge-type structure, mean agglomerate size, and specific surface area values) governs precursor evolution processes being similar. xCaO-(100-x)ZrO_2 precursors (x = 9, 12, and 15 mol.%) obtained by freeze-drying can be used for futher nanoceramics fabrication suitable as membranes for high temperature in-situ oxygen sensors.

ACKNOWLEDGEMENTS

This research work was supported by the special President's scholarship for young scientists (research project CP-1967.2016.1). SEM was performed at the Research park of St. Petersburg State University Center for Geo-Environmental Research and Modeling (GEOMODEL)». STA was performed at the Research park of St. Petersburg State University Center for Thermogravimetric and Calorimetric Research. BET research was performed at the Research park of St. Petersburg State University Center for Innovative Technologies of Composite Nanomaterials.

REFERENCES

[1] V.S. Galkin, V.G. Konakov, A.V. Shorohov and E.N. Sovovieva // *Rev. Adv. Mater. Sci.* **10** (2005) 353.

[2] H.J.M. Bouwmeester and A.J. Burgraaf, In: *Fundamentals of Inorganic Membrane Science and Technology*, ed. by A. J. Burggraaf and L. Cot (Elsevier, 2001).

[3] M.O. Zacate, L. Minervini, D.J. Bradfield, R.W. Grimes and K.E. Sickafus // *Solid State Ionics* **128** (2000) 243.
[4] S.P.S. Badwal // *Solid State Ionics* **52** (1992) 23.
[5] N. Mahato, A. Gupta and K. Balani // *Nanomat. and Energy* **1** (2012) 27.
[6] Y.W. Chang and C.C. Lin // *J. Am. Ceram. Soc*. **93** (2010) 3893.
[7] W.E. Lee and R.E. Moore // *J. Am. Ceram. Soc.* **81** (1998) 1385.
[8] O.Yu. Kurapova and V.G. Konakov // *Rev. Adv. Mater. Sci.* **36** (2014) 176.
[9] L. Qian and H. Zhang // *J. Chem. Technol. Biotechnol.* **86** (2011) 172.
[10] Z. Zhao, D. Chen and X. Jiao // *J. Phys. Chem. C* **111** (2007) 18738.
[11] S. Deville // *Adv. Eng. Math*. **10** (2008) 155.
[12] J. Beirowski, S. Inghelbrecht and A. Arien // *J. of Pharm. Sci.* **100** (2011) 1958.
[13] J. Mouzon and O. Oden // *J. Amer. Cer. Soc*. **89** (2006) 3094.
[14] A. Lasalle, C. Guizard, J. Leloup, S. Deville, E. Maire, A. Bogner, C. Gauthier, J. Adrien and L. Courtois // *J. Am. Ceram. Soc*. **95** (2012) 799.
[15] S.W. Sofie and F. Dogan // *J. Am. Ceram. Soc.* **84** (2001) 1459.
[16] V.S. Stubican and S.P. Ray // *J. Am. Ceram. Soc*. **60** (1977) 535.
[17] V.G. Konakov, S.N. Golubev, O.Yu. Kurapova, N.V. Borisova and V.M. Ushakov // *Bull. St Petersburg University* **4** (2012) 49.
[18] J. Rouquerol, F. Rouquerol, P. Llewellyn, G. Maurin and K.S. Sing, *Adsorption by powders and porous solids: principles, methodology and applications. 2nd edition* (Academic press, 2013).
[19] R. Stevens // *Magn. Electron Publ.* **5** (1986) 56.
[20] L. Barin and O. Knacke, *Thermochemical properties of inorganic substances* (Springer, 1973).
[21] A.S. Sinitsky, V.A. Ketsko and I.V. Penti // *Russ. J. Inorg. Chem*. **48** (2003) 484.
[22] J.P. Oliver // *Journal of Porous Materials* **2** (1995) 9.
[23] D.A. Ivanov-Pavlov, V.G. Konakov, E.N. Solovieva, V.M. Ushakov and N.V. Borisova // *Journal of Nano Research* **6** (2009) 35.
[24] V.G. Konakov, S. Seal, E.N. Solovieva, S.N. Golubev, M.M. Pivovarov and A.V. Shorochov // *Rev. Adv. Mater. Sci.* **13** (2006) 71.